2

THE STUDY OF RADIATION DAMAGE IN METALS BY POSITRON ANNIHILATION*

W. B. Gauster
Sandia Laboratories
Albuquerque, NM 87115

CONF-771110--5

ABSTRACT

Positron annihilation is a sensitive technique for probing defects in metals and it has recently been shown to be a valuable tool for the study of radiation damage. After an introduction to the three basic experimental methods (angular correlation, Doppler broadening, and lifetime measurements), the interaction of positrons with lattice defects is reviewed. Results for the annealing of damage after low temperature irradiation are used to show that positron annihilation has provided new information on annealing kinetics. The role of positron techniques in characterizing complex defect structures resulting from high-temperature neutron irradiation is reviewed and the possible utility of positron annihilation as a nondestructive monitor of property changes is pointed out.

*This work supported by the United States Department of Energy under Contract AT(29-1)789.

I. INTRODUCTION

It has been recognized for about ten years now that positron annihilation in solids is sensitive to defects. Certain characteristics of the annihilation radiation depend sensitively on the concentration of vacancies or other "open-volume" defects in the sample. The past five years have seen the start of a systematic exploitation of this effect as an experimental tool. A prominent area of application is the study of radiation damage in metals. Although the field is quite young, positron annihilation has already had impact in terms of providing improved understanding of annealing kinetics as well as in the characterization of complex defect structures.

We will begin with a discussion of the physics of positron annihilation, leading up to the interaction of positrons with defects. A review of experimental work will emphasize comparison with other techniques and summarize results obtained for annealing of damage after particle irradiation.

II. PHYSICS OF POSITRON ANNIHILATION

Positrons are most commonly obtained from sources external to the sample under study. Suitable β^+ emitters are produced in a variety of reactions and are commercially available. The positrons emitted have a distribution of energies up to a maximum value that determines their deepest penetration in a metal. Typical mean depths are 10 to 100 μm, so the positrons are implanted in the bulk of the samples. Table I is a listing of

the most commonly used source isotopes, together with the production reactions, the half-lives of the resulting nuclei and the maximum energies of the emitted positrons.[1]

Positrons entering a metal rapidly lose most of their kinetic energy by collisions with ions and electrons, and finally phonons, reaching thermal velocities in a few times 10^{-12}s.[2,3] The thermalized positrons may be represented by Bloch waves moving in the array of ion potentials. Being anti-particles of electrons, positrons will annihilate with electrons, most commonly in a 2γ process, after a lifetime of typically several 10^{-10}s in a metal. Coulomb interactions repel the positrons from positive ion cores, so that they annihilate primarily with conduction electrons. The positrons themselves occupy states at the bottom of the positron conduction band at the time of decay. In detailed discussions of the annihilation characteristics, the charge screening around the positrons plays an important role.

For some purposes it is useful to represent the behavior of the thermalized positron by a diffusion constant D, without specifying the microscopic processes. Then, in the lifetime τ, the positron will cover a distance

$$\ell = \sqrt{2D\tau} \approx 10^3 \text{ Å} , \qquad (1)$$

which gives a measure of the volume sampled before decay. This point will be important in the discussion of positron-defect interactions (trapping model).

The radiation emitted in the annihilation process yields information about the electron distribution at the site of the

decay. Let $\Gamma_i(\vec{p})d^3\vec{p}$ equal the probability of annihilation with the i^{th} electron, for a photon pair momentum in $d^3\vec{p}$ about $\vec{p}$ (two-photon annihilation). If $\Psi_i(\vec{r})$ is the wavefunction of the i^{th} electron and $\Psi_+(\vec{r})$ is the wavefunction of the positron,

$$\gamma_i(\vec{p})d^3\vec{p} = \frac{\pi r_o^2 c}{(2\pi)^3} \left| \int \Psi_i(\vec{r})\ \Psi_+(\vec{r}) e^{-i\vec{p}\cdot\vec{r}} \right|^2 d^3\vec{r} \quad , \tag{2}$$

where r_o is the classical electron radius and c the speed of light. The total annihilation rate (or reciprocal positron lifetime) is obtained by summing over all occupied electron states and photon momenta:

$$\Gamma = \sum_i \Gamma_i = \sum_i \int \gamma_i(\vec{p})d^3\vec{p} \quad . \tag{3}$$

Because the positron occupies its lowest energy state, its contribution to the total momentum is negligible. Thus Γ depends primarily on the momentum distribution of the electrons at the site of decay, and that is the key to the utility of the positron annihilation technique. Several of the general references listed at the end of the paper contain detailed theoretical discussions.

Figure 1 shows schematically the three techniques used in positron annihilation studies. The positron lifetime is a function of the electron density, as seen from Equation (3). Measurements of the positron lifetime can be done if a source is used, such as ^{22}Na, that emits a "marker γ" in coincidence with the positron. The marker is used to start a clock, and one of the annihilation γ's to stop it.

Both angular correlation and Doppler broadening yield information about electron momenta. If the positron and the electron with

which it annihilates were at rest at the time of decay, the two photons emitted would be at exactly 180° with respect to each other in order to conserve momentum. In fact, however, the positron is essentially at rest but the electron is not. Thus the directions of the γ's deviate slightly from 180° by an angle θ. Let the z- component of the pair momentum be $p_z = \hbar k_z$. For small angles $p_z = mc\theta$, where m = electron mass. The angular correlation counts $N(p_z)$ are given by

$$N(p_z) = \iint_{-\infty}^{+\infty} \Gamma_i(p_x, p_y, p_z)\, dp_x\, dp_y \quad . \tag{4}$$

It is readily shown that for a spherical Fermi surface (free electron approximation), the resulting distribution is an inverted parabola. In metals the measured distribution consists of this parabolic part, referred to as the conduction electron contribution, superimposed on a broader portion going to higher momenta and often represented by a Gaussian function. Most of the latter is attributed to the overlap of positron wavefunctions with the wavefunctions of tightly bound electrons and is referred to as the core contribution. [illegible] detailed theoretical discussions.

Doppler broadening measurements are accomplished by looking at the annihilation photons head-on with an energy-resolving detector. Now the electron momentum component (p_x) parallel to the direction of the emitted photon is resolved, rather than the perpendicular component (p_z) measured by angular correlation. If E_0 = 511 keV is the rest energy and m_0 the rest mass of the electron,

$$E = E_0 \pm \Delta E = m_0c^2 \pm \frac{c}{2} p_x \quad ; \text{ if } v << c \quad . \tag{5}$$

For an electron energy of 10 eV, the order of magnitude of the

Fermi energy, $2\Delta E = 3$ keV. The best resolution of Ge(Li) detectors is about 1.1 keV at 511 keV, so the momentum resolution $\Delta p_x \approx \frac{1}{3} k_F$. In angular correlation experiments an order of magnitude better resolution is readily obtained. However, data acquisition for Doppler broadening measurements is considerably faster and the experimental geometry simpler.

III. TRAPPING MODEL

After several independent sets of experiments had shown that positron annihilation is sensitive to defects in metals, a "trapping model" formulated by Brandt[5] was applied to vacancies in metals by Bergersen and Stott[6] and by Connors and West.[7] A discussion of the trapping process in terms of trapping potentials was given by Hodges,[8] and a very complete treatment of the trapping model and related problems is found in a review by Seeger.[9]

The experimental observation underlying the discussion of trapping is that positron annihilation characteristics change as a function of increasing defect concentration, both for defects in thermal equilibrium and for nonequilibrium defects introduced by deformation, quenching, or irradiation. Positron lifetimes become greater, and curves measured by angular correlation or Doppler broadening become more sharply peaked. These effects begin for atomic concentrations of defects between 10^{-7} and 10^{-6}, and saturation occurs for concentrations of approximately 10^{-4}. They have been seen for many, but not all metals. The observations suggest that positrons, in the time between thermalization and decay, can be trapped at defects. Once a positron is localized at an "open-volume" defect, it sees a reduced charge density, resulting in a greater lifetime.

Moreover, its wavefunction will overlap less with the wavefunctions of core electrons than when it is at an interstitial site and more with the wavefunctions of the conduction electrons that fill the defect volume. This results in an enhancement of the peak of the angular correlation (or Doppler broadening) curve, that peak being associated with conduction electrons. The onset of the effect will occur when the defect concentration is such that the positron will find a defect in the volume sampled before decay (Eq. 1). An example of the effect in angular correlation measurements is shown in Figure 2.

We assume that no detrapping occurs, i.e., each positron is trapped only once. We let λ_t be the decay rate of a trap, λ_f the decay rate in the perfect lattice, c the concentration of traps, μc the trapping rate of positrons, n_t the number of trapped positrons and n_f the number of free positrons. The number of free positrons can be reduced both by decay and by trapping; the number of trapped positrons is increased by trapping and reduced by decay:

$$\frac{dn_f}{dt} = -\lambda_f n_f - \mu c\, n_f$$
$$\frac{dn_t}{dt} = -\lambda_t n_t + \mu c n_f \quad . \tag{6}$$

The solutions are

$$n_f(t) = n_f(0)\exp[-(\lambda_f + \mu c)t]$$
$$n_t(t) = \frac{\mu c n_f(0)}{\lambda_t - \lambda_f - \mu c}\left\{\exp[-(\lambda_f \quad t] - \exp[-\lambda_t t]\right\} \quad . \tag{7}$$

If we let p_t = fraction of annihilations co[illegible] from traps, then

$$p_t = \frac{1}{n_t + n_f}\int_0^\infty \lambda_t n_t(t)dt = \frac{\mu c}{\lambda_f \quad \mu c} \quad . \tag{8}$$

Equation (8) allows one to model the observed saturation effects. Let F be a measured parameter, such as the mean lifetime, a normalized point (usually the peak) on the angular correlation curve, or a Doppler broadening lineshape parameter (usually the peak divided by the area), and let F_f and F_t be the corresponding quantities for the cases of all positrons annihilating in the bulk and from traps, respectively. Then

$$F = F_f(1 - p_t) + F_t\, p_t \quad ,$$

or

$$\frac{F - F_f}{F_t - F_f} = \frac{\mu c}{\lambda_f + \mu c} \quad . \tag{9}$$

The above equations are used to extract the vacancy formation enthalpy from measurements of positron annihilation as a function of sample temperature.[10] The equilibrium vacancy concentration c(T) is given by $c = B \exp(-\phi/k_B T)$, where ϕ is the formation enthalpy and k_B Boltzmann's constant. With rising sample temperature, c increases from a value for which no positrons find vacancies to one for which all positrons decay from vacancy traps. A characteristic "S" curve is measured for F, and a fit of Equation (9) to the data yields ϕ.

For radiation damage studies, the parameter μ(trapping rate per trap) becomes particularly important. The parameter F is a function not only of trap concentration, but also of trapping rate μc. Further, it is plausible that $(F_t - F_f)$ will be different for different trapping sites, i.e., vacancies, vacancy clusters, voids, dislocation cores. In the discussion of the trapping model it was assumed so far that there is only one type

of trap. This need not be so, and there are cases for which several types of trapping sites can be resolved or changes in the dominant traps can be identified.

IV. EXPERIMENTAL TECHNIQUES

The experimental arrangements for the three measurement techniques are shown in Figures 3, 4, and 5, and we discuss each in turn.

a. Lifetime

Lifetime measurements rely on the use of sources, such as ^{22}Na or ^{44}Sc, that emit a gamma ray simultaneously with the positron. The time delay between the detection of the prompt photon (1.28 MeV for the case of ^{22}Na) and the detection of the 0.511 MeV annihilation photon is recorded by a fast-slow coincidence apparatus, as shown in Figure 3. A sandwich arrangement of samples and source is used to ensure that all positrons are stopped in sample material, and the detectors (plastic scintillators) are positioned close to the samples. The measured lifetimes of a few times 10^{-10} s are near the limit of resolution of the apparatus.

A fit to the lifetime spectrum is usually made by computer, using a small number of exponential decay components of the form $\exp(-\lambda t)$. Alternatively, one "mean lifetime" is extracted from the data. While it is often difficult to resolve several lifetimes accurately, in those cases where it can be done valuable information is obtained, for example about the emergence of a new trapping center after a given radiation dose or annealing treatment.

b. Angular Correlation

Figure 4 shows a typical angular correlation apparatus in the "long-slit" geometry. Sources of several mCi to several Ci are used, as opposed to typically 10 to 100 μCi for lifetime and Doppler broadening. The sources are usually external to the sample, and well shielded from the detectors. Internal sources have, however, been used successfully as well, for example by activating Cu samples by irradiation with thermal neutrons to produce the isotope ^{64}Cu.[11]

In the long-slit geometry, one dimension of the detector slit (out of the paper in Figure 4) is much greater than the slit width, and also much greater (in milliradians) than the width of the angular correlation curve. This is equivalent to integrating the angular correlation counts over two components of momentum, and determining only the transverse momentum component p_z of the photon pair (See Equation (4)). Very precise measurements, involving an angular resolution of 0.1 milliradians and accumulated counts of 10^5 per position, can be made.

The long-slit geometry is the one that has been used so far in defect studies, including radiation damage. For Fermi surface studies, however, more information is obtained in the crossed slit configuration.[11] There have been very exciting developments recently in the area of multi-detector systems,[12,13] allowing two-dimensional angular correlation measurements. Such systems are under development at several laboratories and it is likely that they will find application in the study of defects.

c. Doppler Broadening

Figure 5 shows a Doppler broadening spectrometer, together with a ^{85}Sr line at 514 keV representing the resolution of the system, and a broadened annihilation line from copper samples. The application of this technique, particularly in metallurgical studies, has grown rapidly in recent years. Despite the limited resolution, corresponding to ~ 4 mr in angular correlation, Doppler measurements have the advantages of shorter counting times, even for relatively weak sources, and of flexibility in geometry. The latter permits samples to be studies in various environmental conditions and holds out the promise of possible applications in nondestructive evaluation.[14] Doppler broadening experiments depend critically on careful stabilization of the electronics. For example, temperature control to ± 0.1°C is required, together with the use of a digital stabilizer or stabilization by software. Recent advances make it possible to obtain intrinsic germanium detectors with energy resolutions equal to those of lithium drifted crystals. The convenience and expected longer life of these detectors should further advance the usefulness of the technique.

V. RADIATION DAMAGE

Before discussing specific experiments involving positron annihilation, it is useful to review some of the fundamental concepts of radiation damage.[15,16] The study of radiation damage can be separated into two areas, represented in Figure 6, showing a displacement cascade, and Figure 7, showing a displacement spike.

In one set of experiments, samples are irradiated under carefully controlled conditions, for example with electrons of MeV energies at liquid helium temperature. The object is to introduce a known density of vacancy-interstitial pairs (Frenkel pairs) at a sample temperature low enough that both types of defects remain immobile. The defect geometry is the result of the displacement cascades produced in the slowing down of all displaced atoms. Subsequently, measurements are carried out on the samples as a function of annealing treatment in order to obtain information about defect kinetics and the geometry and stability of resulting defect clusters.

Figure 7 represents a more complex situation, a vacancy-rich region surrounded by a shell of material rich in interstitials. Such displacement spikes can result from irradiation by high-energy particles at low temperatures, and may not remain stable as the sample temperature is raised. The figure is intended here to be representative of the more complex defect structures resulting, for example, from high temperature exposure to a reactor environment. The goal of an important area of study is to characterize the microstructure resulting from irradiation and relate it to observed macroscopic property changes such as swelling, embrittlement or radiation-induced creep.

For many metals, the isochronal annealing after low temperature irradiation has been observed to take place in several discrete steps, each step occurring in a well defined temperature region. The goal of a large number of experiments in recent years has been to provide detailed information about the

processes reponsible for these recovery stages. The results have been interpreted in terms of two models, which are discussed critically in References 17 and 18.

The development of diffuse x-ray scattering techniques[19] has made it possible to determine defect configurations and to detect clustering, primarily for interstitials. Positron annihilation complements these techniques because of its sensitivity to vacancies and vacancy clusters. Thus it is particularly interesting to examine annealing stage III which is attributed in one model to the motion of vacancies to sinks and to vacancy clusters, and in the other model to the movement of interstitials. This is one of the areas to be disucssed below.

VI. POSITRON ANNIHILATION EXPERIMENTS

Since the first measurements on electron-irradiated platinum[20] and iron[21] by angular correlation, positron annihilation has been widely used in radiation damage studies. Particular excitement was generated by two short papers in Nature,[22,23] in which it was reported that the presence of voids due to fast neutron irradiation of molybdenum at 650°C caused an increase of the angular correlation peak count rate by about 65%, with corresponding effects on the Doppler broadening of the annihilation line and on the observed lifetime spectrum. The authors pointed out the promise of the technique as a viable early warning system for impending failure of reactor components.

For the purposes of discussion it is useful to group the work done more recently into several categories. One area that

has received considerable attention is the interpretation of annealing stages, referred to briefly in the preceding section.

a. Stage III

After the large effects due to high-temperature neutron irradiation of molybdenum had been observed,[22,23] studies of the annealing behavior after neutron irradiation at about 60°C of the same metal were undertaken.[24,25] It was found that voids can be produced not only by irradiation at elevated temperatures, but also during annealing following low temperature irradiation. This result was later confirmed by electron microscopy,[26] and underlined the extreme sensitivity of the positron annihilation technique. During stage III (150-350°C) a lifetime component was observed to increase, as did the Doppler broadening lineshape parameter. It was concluded that the migration of first divacancies and then monovacancies led to the formation of small vacancy clusters.

In order to investigate stage III behavior under cleaner experimental conditions, the annealing of molybdenum irradiated with 10 MeV electrons at 50°C was studied, in combination with liquid helium electrical resistivity measurements.[27,28] Both lifetime and angular correlation were measured and a very careful data analysis was carried out. It was again deduced that vacancy clustering took place in stage III, and the conclusion was strengthened by the electron-microscopic observation of some three-dimensional voids.

The results of neutron and electron-irradiation experiments on molybdenum were recently summarized concisely by Petersen.[29] In particular, on the basis of arguments concerning differences in sink geometries, he concluded that the experiments of Petersen, Nielsen and Thrane[30] on both single crystal and polycrystal samples show that vacancies migrate in stage III.

A very careful study of low temperature electron-irradiated copper was carried out by Mantl and Triftshäuser.[31] They observed a strong increase of the lineshape parameter in stage III, which they interpreted as being due to small three-dimensional vacancy clusters that form once the vacancies are able to migrate. A parameter R, defined previously,[32] was calculated from the measured lineshapes as a function of annealing temperatures. Under certain assumptions, this parameter is independent of defect concentration and characterizes the positron trapping site. It was found that during stage III R changed from a value that had been observed for vacancies in thermal equilibrium to one considerably higher. High R values had also been observed for aluminum samples containing voids.

Further support for the vacancy clustering interpretation was obtained from results, reported in the same paper, on some quenched gold samples. Here, too, an increase of lineshape parameter and of the R parameter was found in stage III. Only vacancies are frozen in by quenching; therefore the similarity of the effects observed for quenched gold and electron-irradiated copper suggests that in the latter case, too, vacancy clustering is the cause of the effect.

It can be argued,[33] however, that the positron annihilation effects observed for electron-irradiated copper might be due to trapping by very small interstitial loops that are formed when self-interstitials begin to migrate. More detailed studies of quenched metals, particularly of copper, are of interest here for comparison with results on irradiated samples. It is not a trivial problem, however, to reliably quench sufficient concentrations of vacancies into samples of the required dimensions.

Recently, the annealing of quenched aluminum single crystals and polycrystals was investigated by Doppler broadening and electrical resistivity,[34] and the results were compared to similar measurements on electron-irradiated aluminum.[35] For the quenched samples, a rise of the lineshape parameter in stage III was seen to correlate directly with the relative magnitude of the lineshape parameter in stage IV, where electron microscopy has shown dislocation loops to be present. Thus it was concluded that the increase of lineshape parameter in stage III was due to the early stages of vacancy clustering, and that some of these clusters eventually grew to form loops that were stable through stage IV. For electron irradiated aluminum, no rise was observed in stage III and consequently no stages IV and V were seen. This means that the interstitial clusters resulting from irradiation followed by annealing through stage II provided such a large concentration of sinks for vacancies that they were all annealed in stage III without clustering.

Similar measurements on quenched copper would be helpful in the interpretation of the data on electron-irradiated copper.

There are some complications in such work on copper that do not enter for aluminum, but in fact measurements on quenched copper are now underway.[36]

The annealing behavior of electron-irradiated copper has also been investigated by positron lifetime.[37] It was found that a long-lifetime component appeared in stage III, the value of which increased even into stage IV. This component was interpreted as being due to three-dimensional vacancy clusters, in agreement with the interpretation of Ref. 31. At high temperatures (above 200°C), it was inferred from the data that two long-lived components exist, one associated with dislocation loops and the other with microvoids, and that these two components annealed out at different temperatures. Similar structure in the high temperature annealing stages has also been seen for neutron irradiated copper, in some work to be discussed next.

b. Stage V

For irradiation temperatures above stage III, neutron damage in copper consists of defect clusters. Various techniques have been used to study this damage, and it was found that the clusters are primarily dislocation loops, of both interstitial and vacancy type.[38] The annealing stage in which these clusters disappear is labeled stage V. Positron annihilation measurements on copper crystals as a function of neutron dose (irradiation temperature ~ 50°C) have shown that positrons are trapped, presumably at the cores of these dislocation loops.[39] Subsequent positron annihilation annealing studies[40] on the same crystals showed a

structure in the annealing curve that had not been observed previously by other techiques (See Figure 8). A sharp rise in the normalized peak count rate was measured in a narrow temperature interval, and was interpreted as being due to trapping of positrons at microvoids that can form when vacancy type dislocation loops become unstable and release vacancies. In fact, the temperature at which the effect was observed corresponds to the irradiation temperature (300°C) above which only very few dislocation loops visible by transmission electron microscopy are produced by self-ion irradiation in copper,[41] presumably because they are thermally unstable.

These findings were confirmed in similar measurements on neutron-irradiated copper by angular correlation and lifetime.[42] Here, however, the peak was not as pronounced. The interpretation given was that some microvoids may form during irradiation, even at a temperature as low as 50°C. The peak seen in Ref. 40 would then be due to the growth of these microvoids after vacancies are released from loops.

In Ref. 40 measurements were reported as well on copper samples doped with ^{10}B and subsequently irradiated with thermal neutrons. The energetic α and Li particles resulting from the reaction $^{10}B(n,\alpha)^{7}Li$ then produced damage, which was seen by electron microscopy to be similar to that produced by fast neutrons. The annealing behavior for this second set of samples followed very closely that for the neutron damaged speciments, the peak occurring at the same temperature. Later, measurements on ^{10}B-doped copper irradiated at a higher temperature (~ 260°C) showed a

much broader peak in the recovery curve, centered near 400°C.[43] This shift in the annealing curve reflects the differences in defect geometry resulting from higher irradiation temperature. The distribution of loop diameters is shifted to larger values,[38,41] and a higher concentration of microvoids is expected.

c. Voids

In high-temperature neutron irradiations, the irradiation temperature can be varied in order to produce different void sizes. In a recent study[44] it was found that the long positron lifetime component for a series of Mo samples containing voids varying in mean radius from 9 Å to 45 Å remained constant to within experimental error. This result is in agreement with theoretical work[45,46] indicating that positron annihilation parameters should depend only weakly on void size for voids containing more than 20 vacancies (i.e., r > 5 Å), although below a critical value the parameters should vary strongly with cluster size. The same conclusions were reached in a independent study also on Mo by another group.[47]

After these findings, the reasons for unusually long lifetimes measured in earlier annealing studies of molybdenum were reexamined. It was determined experimentally[48] that impurities introduced during the annealing in a gas atmosphere can strongly affect the measured lifetimes.

The screening of the Coulomb interaction between a position and an electron by valence electrons ordinarily prevents the

formation of a positron-electron bound state (positronium) in a metal. There has been some interest in the question whether positronium could, however, be formed in voids in a metal lattice. The early work on voids in molybdenum[22,23] included experiments to test for the formation of positronium in the voids. The negative result implied a positronium-positron ratio of less than 3%. More recently, using a 3 γ detection technique, some evidence of positronium formation at voids in molybdenum was obtained,[49] indicating that 1.3% of the positrons were decaying from positronium by the 3 γ process.

Annealing of voids produced in molybdenum by neutron irradiation at 600°C was investigated in lifetime studies by Hinode et al.[50] A clearly resolvable long-lifetime component indicated the presence of voids after irradiation, even though they apparently did not grow to sizes visible in the electron microscope until after annealing at 800°C. Also, from the high-temperature annealing behavior an additional intermediate lifetime component was observed and attributed to dislocation loops.

Recently, both lifetime and Doppler broadening measurements on molybdenum which had been neutron irradiated at high temperatures up to 1500°C were reported.[51] The measured lineshape parameter and a long lifetime component both correlated well as a function of irradiation temperature with the predicted swelling based on measurements by other techniques. The drop at high temperatures was, however, slower for the positron curves, in agreement with the finding that positron annihilation is more sensitive to low concentrations of open-volume defects than other

techniques. Changes in the short lifetime component found at intermediate irradiation temperatures were tentatively attributed to trapping at dislocation loops.

Studies of voids in aluminum began with angular correlation measurements by Triftshäuser et al,[52] on single crystals neutron irradiated to high fluences at 55°C. The measured curve agreed with one calculated on the assumption that the positrons are annihilated at void surfaces. The void trapping effect disappeared after annealing at 325°C.

Subsequent lifetime measurements on a similar aluminum crystal, irradiated under the same conditions, supported the model of positron states at the void surfaces.[53] No evidence for positronium formation was found. Further detailed studies of the same system by positron lifetime and angular correlation, as well as small angle x-ray scattering,[54] were interpreted in terms of a model in which positrons are trapped both at voids and at other defects. These other complexes were tentatively identified as vacancy clusters bound to transmutation-produced silicon. The ability to resolve two long lifetime components with relative contributions that vary differently with annealing temperature illustrates the utility of the lifetime technique.

Helium bubble formation in aluminum after injection of 50 MeV alpha particles was traced by positron lifetime measurements after isochronal annealing steps.[55,56] The results of a comprehensive study, including electron microscopy, were consistent with the assumption that the helium rapidly occupies substitutional sites and that this substitutional helium is a trapping site for

positrons. It was found that the helium begins to migrate near 100°C and agglomerates up to about 250°C. Bubble growth occurs principally between 300 and 600°C.

There has also been a study by lifetime measurements of the damage produced in aluminum by proton bombardment.[57] In order to simulate (n,α) processes induced by fast neutron irradiation, the proton bombardment was preceded by injection of ^{3}He ions. A long lifetime component, evidence of void formation, was observed. Simulation of neutron damage by ion bombardment is attractive because of the short times required to obtain high numbers of displacements per atom. Often the depth to which such damage is produced is very small. For this reason, the low energy positron beams which have recently been developed[58,59] will find application in such studies.

Void formation has also been investigated in neutron irradiated nickel single crystals[60] and polycrystals[61] by angular correlation. In both cases, the positron source was the isotope ^{58}Co produced by the reaction $^{58}Ni(n,p)^{58}Co$ in the sample itself. In Ref. 61 it was found that a fairly large effect persisted even after annealing above 1100°C. This was attributed to small voids stabilized by gas impurities, too small to have been seen by electron microscopy.

d. Iron and Zirconium

Finally, we discuss separately two experiments on the annealing of irradiated iron and zirconium, respectively. In the work on iron,[62] purified samples and specimens doped either with carbon

or with nitrogen were neutron irradiated at 20K. Angular correlation was measured at 77K after annealing steps between 100K and 680K. A comparison of the positron annihilation results with internal friction data showed that the impurities interact with vacancies. It was concluded that carbon-vacancy and nitrogen-vacancy complexes still act as trapping centers for positrons. At the highest annealing temperatures the complexes dissociated and complete recovery was observed.

The lifetime and angular correlation measurements on electron-irradiated α-zirconium[63] deal with a particularly difficult system. The specimens were irradiated at approximately 300K, and measurements were done as a function of isochronal annealing steps. The relatively high impurity levels of the material are expected to play a large role in the recovery processes, and in fact for the less pure of the two samples an almost continuous recovery spectrum was observed.

VII CONCLUSIONS

The work reviewed here shows clearly that positron annihilation can provide important new information on radiation damage of metals, particularly when combined with other techniques. The extreme sensitivity of the method has made it possible to follow vacancy interactions when the clusters are too small to be observed electron-microscopically. This has resulted in an improved understanding of defect recovery stages and void formation and growth phenomena. That same sensitivity, as shown for

example in the swelling work, suggests the application of positron annihilation as a nondestructive monitor of radiation damage to component materials.

REFERENCES

1. A. N. Goland in Fundamental Aspects of Radiation Damage in Metals, Mark T. Robinson and F. W. Young, Jr., eds., USERDA CONF-751006, p. 1107 (1976).
2. G. E. Lee-Whiting, Phys. Rev. 97, 1557 (1955).
3. J. P. Carbotte and H. L. Arora, Can. J. Phys. 45, 387 (1967).
4. W. Brandt, Appl. Phys. 5, 1 (1974).
5. W. Brandt in Positron Annihilation, A. T. Stewart and L. O. Roelling, eds., (Academic Press, New York 1967) pp. 179-181
6. B. Bergersen and M. J. Stott, Solid St. Commun. 7, 1203 (1969).
7. D. C. Connors and R. N. West, Phys. Lett. 30A, 24 (1969).
8. C. H. Hodges, Phys. Rev. Lett. 25, 284 (1970).
9. A. Seeger, Appl. Phys. 4, 183 (1974).
10. W. Triftshäuser and J. D. McGervey, Appl. Phys. 6, 177 (1975).
11. K. Fujiwara and O. Sueoka, J. Phys. Soc. Japan 21, 1947 (1966).
12. W. Triftshäuser, Second International Conference on Positron Annihilation, Kingston, Ontario, Canada, 1971 (unpublished).
13. S. Berko and J. Mader, Appl. Phys. 5, 287 (1975).
14. W. B. Gauster, J. Nucl. Mat. 62, 118 (1976).
15. M. W. Thompson, Defects and Radiation Damage in Metals (University Press, Cambridge 1969).
16. H. S. Rosenbaum in Treatise on Materials Science and Technology, H. Herman, ed., (Academic Press, New York 1975) Vol. 7.
17. W. Schilling in Reference 1, p. 470.
18. A. Seeger, ibid., p. 493.
19. P. Ehrhart, H.-G. Haubold, and W. Schilling in Festkörperprobleme (Advances in Solid State Physics), H. J. Queisser, ed., Pergamon/Vieweg, Braunschweig 1974), Vol. 14, p. 87.

20. J. H. Kusmiss, C. D. Esseltine, C. L. Snead, Jr., and A. N. Goland, Phys. Lett. 32A, 175 (1970).

21. C. L. Snead, Jr., A. N. Goland, J. H. Kusmiss, H. C. Huang, and R. Meade, Phys. Rev. B3, 275 (1971).

22. O. Mogensen, K. Petersen, R. M. J. Cotterill and B. Hudson, Nature 239, 98 (1972).

23. R. M. J. Cotterill, I. K. MacKenzie, L. Smedskjaer, G. Trumpy and J. H. O. L. Träff, Nature 239, 99 (1972).

24. K. Petersen, N. Thrane, and R. M. J. Cotterill, Phil. Mag. 29, 9 (1974).

25. K. Petersen, M. Knudsen, and R. M. J. Cotterill, Phil. Mag. 32, 417 (1975).

26. K. Petersen, J. H. Evans, and R. M. J. Cotterill, Phil. Mag. 32, 427 (1975).

27. J. H. Evans and M. Eldrup, Nature 254, 685 (1975).

28. M. Eldrup, O. E. Mogensen, and J. H. Evans, J. Phys. F: Metal Physics 6, 499 (1976).

29. K. Petersen, Phil. Mag. 36, 385 (1977).

30. K. Petersen, B. Nielsen, and Thrane, Phil. Mag. 34, 693 (1976).

31. S. Mantl and W. Triftshäuser, Phys. Rev. Lett. 34, 1554 (1975).

32. W. Triftshäuser, Phys. Rev. B 12, 4634 (1975).

33. A. Seeger, Phys. Lett. 58A, 481 (1976).

34. W. R. Wampler and W. B. Gauster, to be published.

35. S. Mantl, Ber. d. KFA Jülich - Nr. 1359 (1976).

36. W. R. Wampler and W. B. Gauster, unpublished.

37. K. Hinode, S. Tanigawa and M. Doyama, Rad. Effects 32, 73 (1977).

38. B. C. Larson and F. W. Young, Jr., J. Appl. Phys. 48, 880 (1977).

39. W. B. Gauster and S. R. Dolce, Solid State Commun. 16, 867 (1975).

40. W. B. Gauster, S. Mantl, T. Schober and W. Triftshäuser in Reference 1, p. 1143.

41. C. A. English, B. L. Eyre and J. Summers, Phil. Mag. 34, 603 (1976).

42. J. H. Evans, O. Mogensen, M. Eldrup and B. N. Singh, Fourth International Conference on Positron Annihilation, Helsingør, Denmark, 1976 (unpublished).

43. W. B. Gauster, unpublished.

44. N. Thrane, K. Petersen and J. H. Evans, Appl. Phys. 12, 187 (1977).

45. P. Hautojärvi, J. Heiniö and M. Manninen, Phil. Mag. 35, 974 (1977).

46. P. Jena, A. K. Gupta, and K. S. Singwi, Solid State Commun. 21, 293 (1977).

47. L. J. Cheng, P. Sen, I. K. MacKenzie and H. E. Kissinger, Solid State Commun. 20, 953 (1976).

48. N. Thrane and J. H. Evans, Appl. Phys. 12, 183 (1977).

49. P. Sen, L. J. Cheng and H. E. Kissinger, Phys. Lett. 53A, 299 (1975).

50. K. Hinode, S. Tanigawa and M. Doyama, J. Nucl. Mat. 66, 212 (1977).

51. R. Grynszpan, K. G. Lynn, C. L. Snead, Jr., A. N. Goland, and F. W. Wiffen, Phys. Lett. 62A, 459 (1977).

52. W. Triftshäuser, J. D. McGervey and R. W. Hendricks, Phys. Rev. B 9, 3321 (1974).

53. K. Petersen, N. Thrane, G. Trumpy and R. W. Hendricks, Appl. Phys. 10, 85 (1976).

54. V. W. Lindberg, J. D. McGervey, R. W. Hendricks and W. Triftshäuser, Phil. Mag. 36, 117 (1977).

55. C. L. Snead, Jr. and A. N. Goland, Phys. Lett. 55A, 189 (1975).

56. C. L. Snead, Jr., A. N. Goland and F. W. Wiffen, J. Nucl. Mat. 64, 195 (1977).

57. U. Engman and B. Holmquist, Rad. Effects 24, 65 (1975).

58. K. F. Canter, A. P. Mills, Jr., and S. Berko, Phys. Rev. Lett. 34, 177 (1975).

59. A. P. Mills, Jr., S. Berko and K. F. Canter, Phys. Rev. Lett. 34, 1541 (1975).

60. M. Hasegawa and T. Suzuki, Rad. Effects 21, 201 (1974).

61. S. Nanao, K. Kuribayashi, S. Tanigawa, and M. Doyama, Mat. Sci. Eng. 18, 285 (1975).

62. M. Weller, J. Diehl, and W. Triftshäuser, Solid State Commun. 17, 1223 (1975).

63. G. M. Hood, M. Eldrup and O. E. Mogensen Rad. Effects 32, 101 (1977).

General References

I. Ya. Dekhtyar, Phys. Reports 9, 243 (1974).

M. Doyama and R. R. Hasiguti, Crystal Lattice Defects 4, 139 (1973).

A. N. Goland, Brookhaven National Laboratory Report 16517 (1972).

A. Seeger, J. Phys. F: Metal Physics 3, 248 (1973).

W. Triftshäuser, in Festkörperprobleme (Advances in Solid State Physics), H. J. Queisser, ed., (Pergamon/Vieweg. Braunschweig 1975) Vol. 15, p. 381

R. N. West, Adv. Physics 22, 263 (1973).

Table 1. Isotopes used as positron sources, with their half-lives, production reactions, and positron end-point energies.

Table 2. Summary of positron annihilation radiation damage studies.

ISOTOPE	HALF-LIFE	POSITRON END-POINT ENERGY E_{max} (MeV)	PRODUCTION REACTIONS
^{22}Na	2.58 y	0.54	$^{25}Mg(p,\alpha)^{22}Na$
$^{44}Ti/^{44}Sc$	47 y	1.47	$^{42}Ca(\alpha,2n)^{44}Ti$
^{55}Co	18.2 h	1.50	$^{58}Ni(p,\alpha)^{55}Co$, $^{56}Fe(p,2n)^{55}Co$
^{57}Ni	36.0 h	0.85	$^{56}Fe(^{3}He,2n)^{57}Ni$
^{58}Co	71.3 d	0.48	$^{58}Ni(n,p)^{58}Co$, $^{55}Mn(\alpha,n)^{58}Co$
^{64}Cu	12.9 h	0.65	$^{63}Cu(n,\gamma)^{64}Cu$
^{65}Zn	245 d	0.33	$^{64}Zn(n,\gamma)^{65}Zn$
[illegible]	275 d	1.88	$^{66}Zn(\alpha,2n)^{68}Ge$
[illegible]	40 h	1.22	$^{69}Ga(d,2n)^{69}Ge$
^{90}Nb	14.7 h	1.50	$^{90}Zr(p,n)^{90}Nb$, $^{90}Zr(d,2n)^{90}Nb$

TABLE 1

TABLE 2. Positron annihilation studies of radiation damage in metals

Sample Material	Category		Reference
Mo	Stage III	neutrons	24,25,26,29,30
		electrons	27,28
Cu	Stage III	electrons	31,37
Aℓ	Stage III	electrons	35
		quenched	36
Cu	Stage V	fast neutrons	40
		^{10}B doped, thermal neutrons	40,43
Mo	voids		22,23,44,47,48,50
Mo	correlation with swelling		51
Aℓ	voids		52,53,54
Aℓ	bubble formation		55,56
Ni	void formation		60,61
Fe	low temperature neutron irradiation		62
A302B steel	low dose neutron irradiation		14

FIGURE CAPTIONS

Figure 1 Schematic representation of the three experimental techniques used in positron annihilation measurements.

Figure 2 Angular correlation curve for iron, with and without irradiation-produced defects. (Ref. 62)

Figure 3 Typical positron annihilation lifetime spectrometer arrangement.

Figure 4 Schematic arrangement of "long-slit" angular correlation apparatus.

Figure 5 Doppler-broadening spectrometer arrangement and example of data.

Figure 6 Displacement cascade

Figure 7 Displacement spike

Figure 8 Annealing characteristics of neutron-irradiated copper as measured by positron annihilation and by integral diffuse x-ray scattering. (Ref. 40)

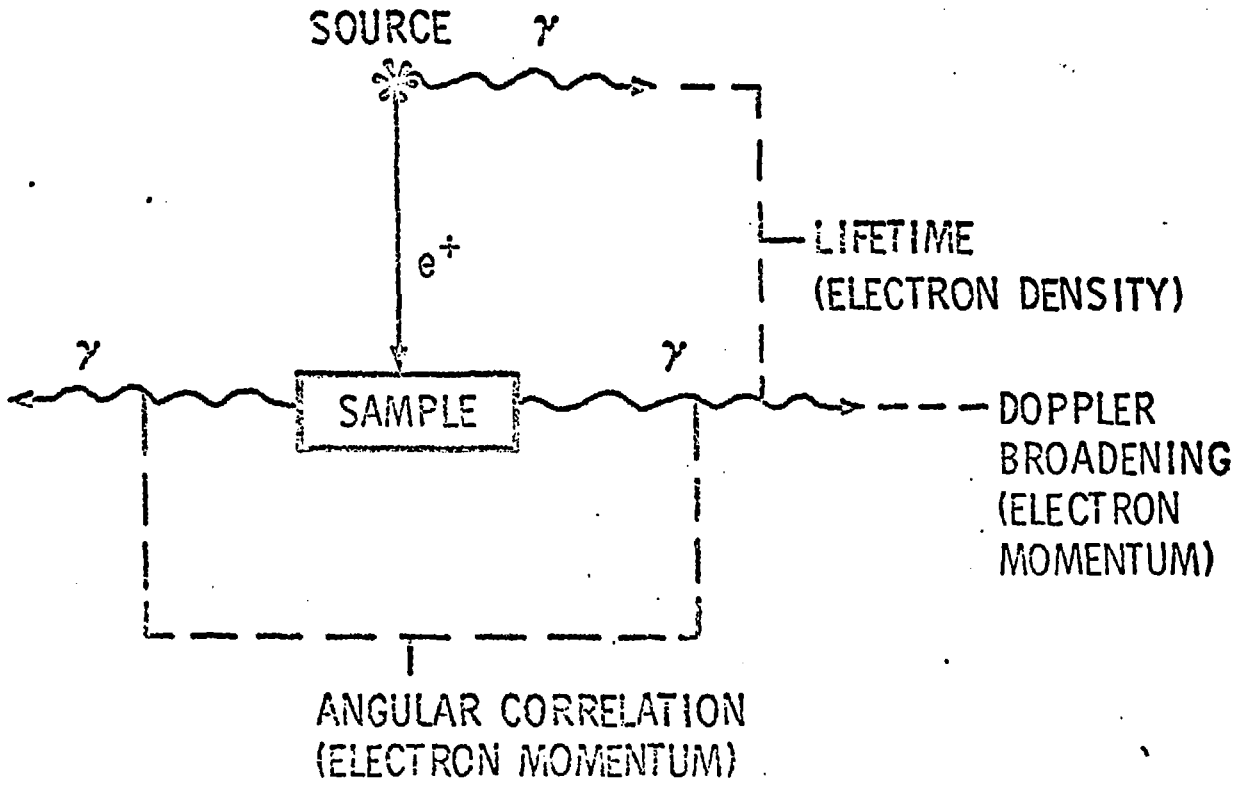
SOURCE
γ
e+
LIFETIME
(ELECTRON DENSITY)
γ
γ
SAMPLE
DOPPLER
BROADENING
(ELECTRON
MOMENTUM)
ANGULAR CORRELATION
(ELECTRON MOMENTUM)

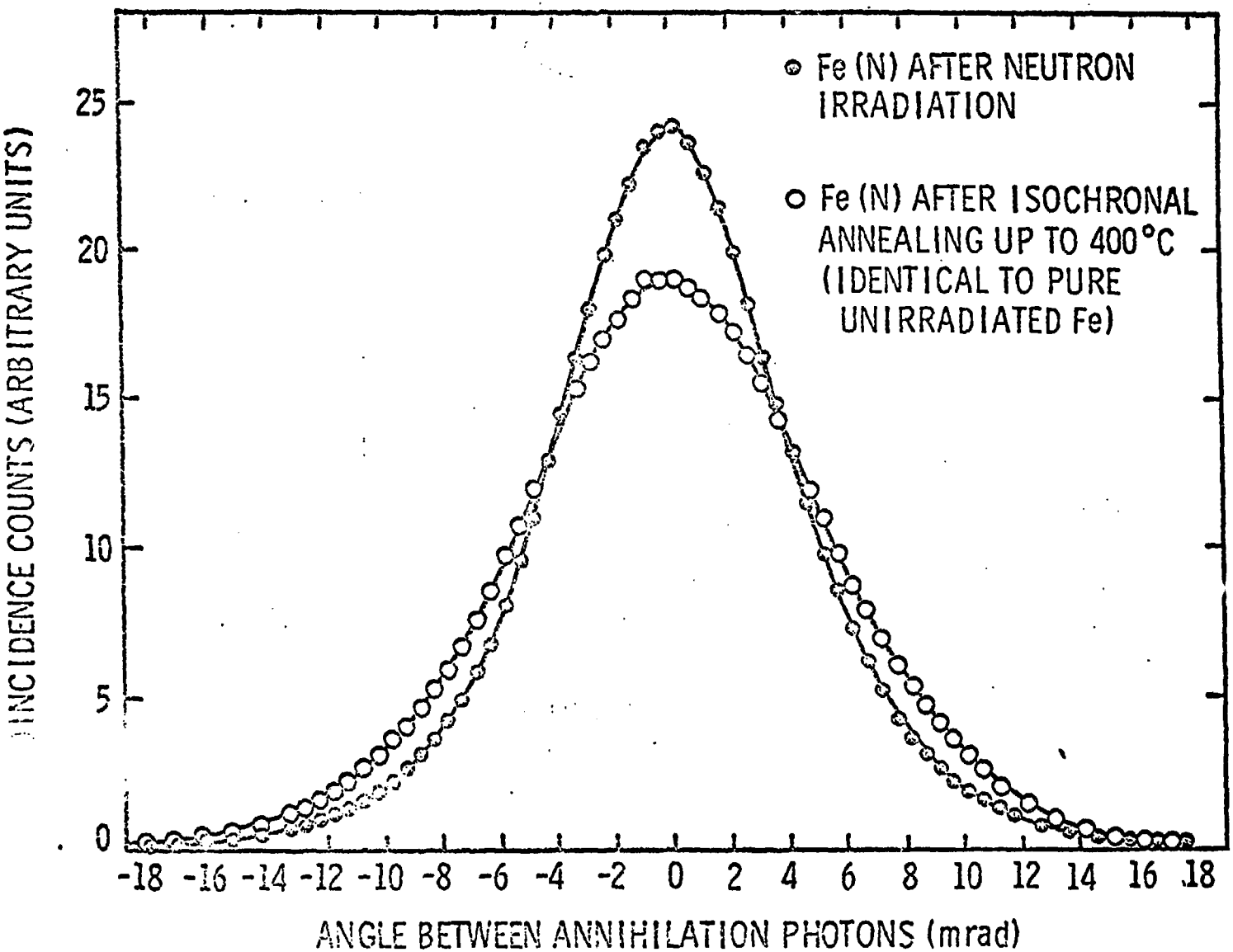

FROM M. WELLER, J. DIEHL AND W. TRIFTSHÄUSER, SOLID STATE COMM. 17, 1223 (1975)

POSITRON ANNIHILATION
LIFETIME

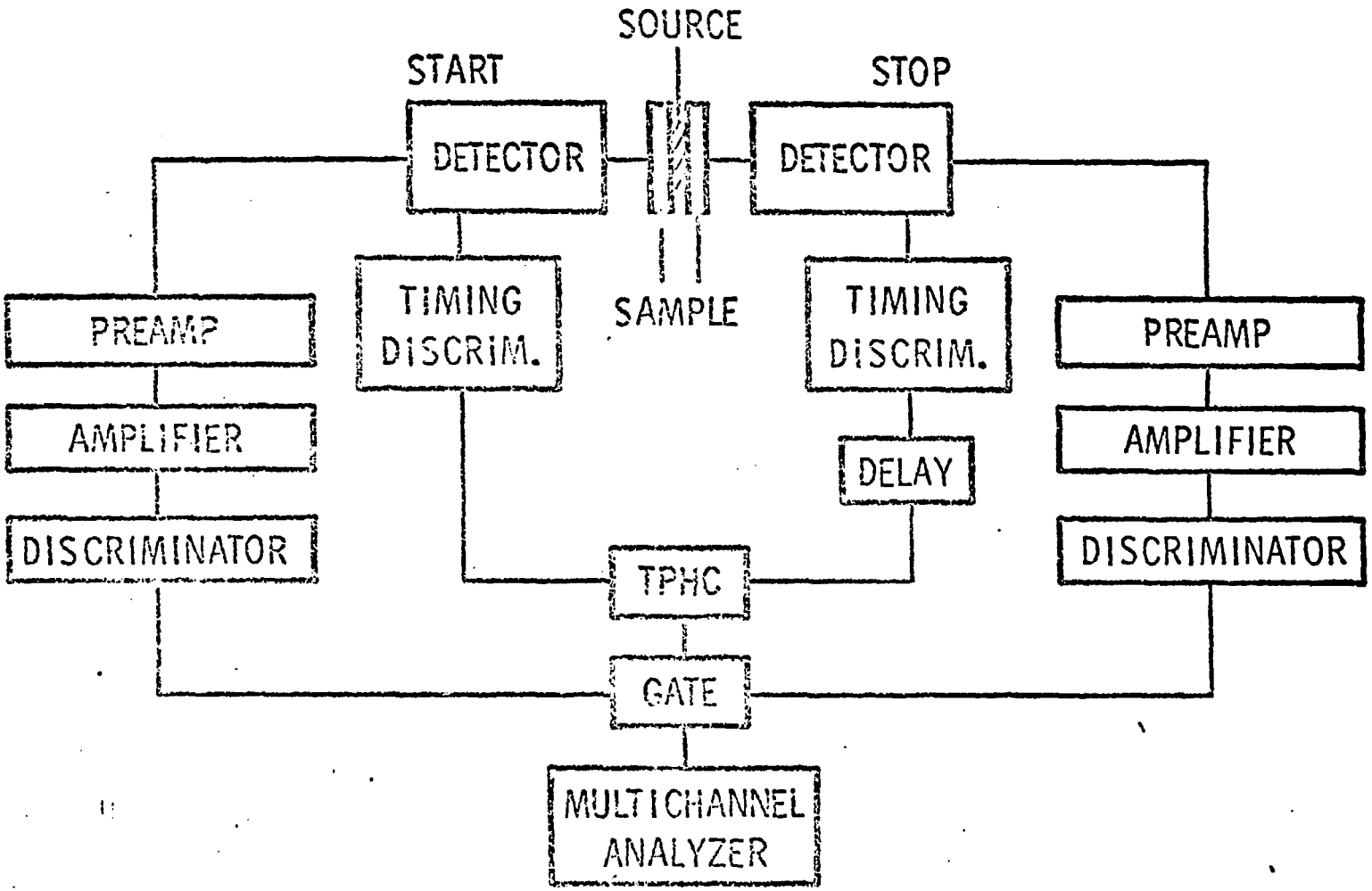

POSITRON ANNIHILATION

ANGULAR CORRELATION

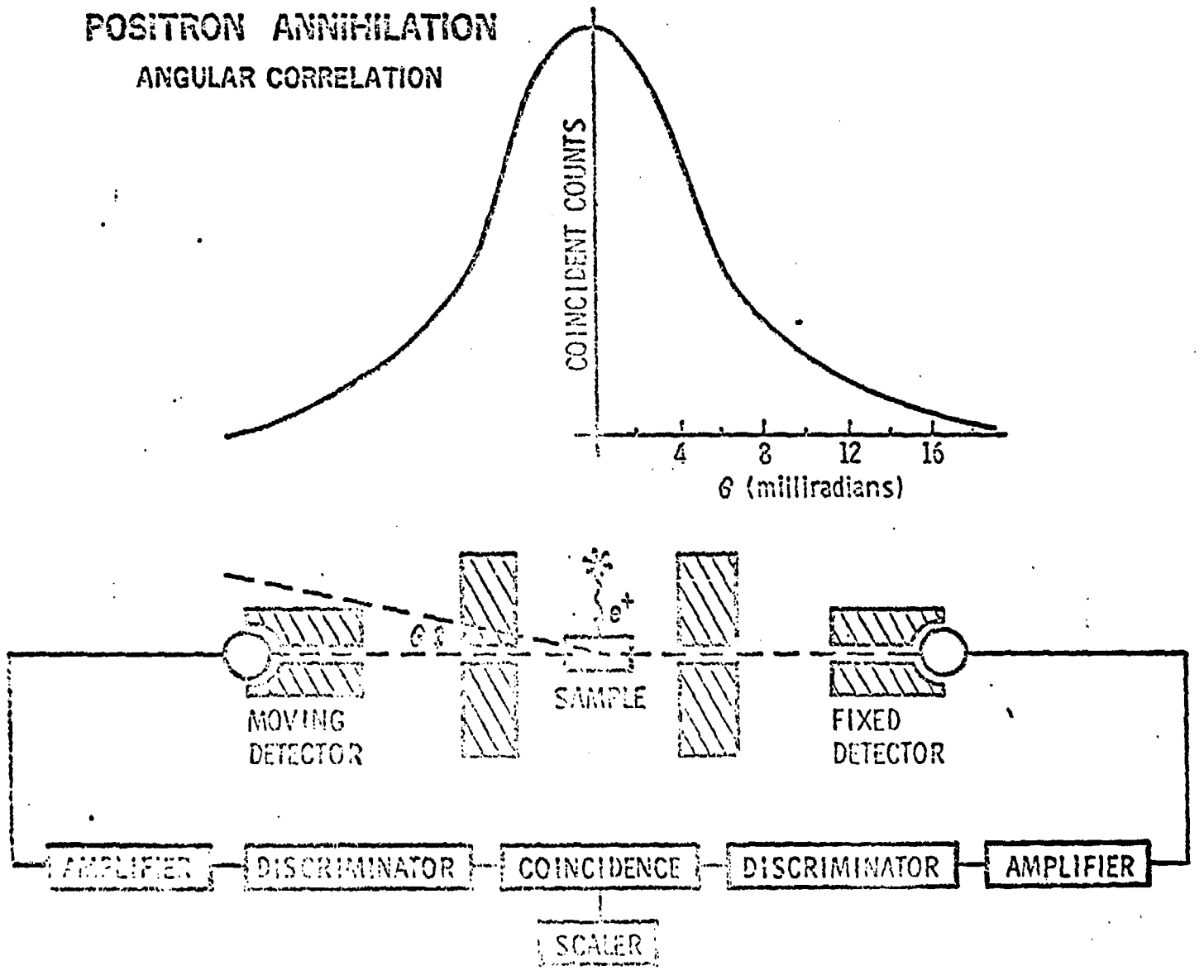

POSITRON ANNIHILATION
DOPPLER BROADENING

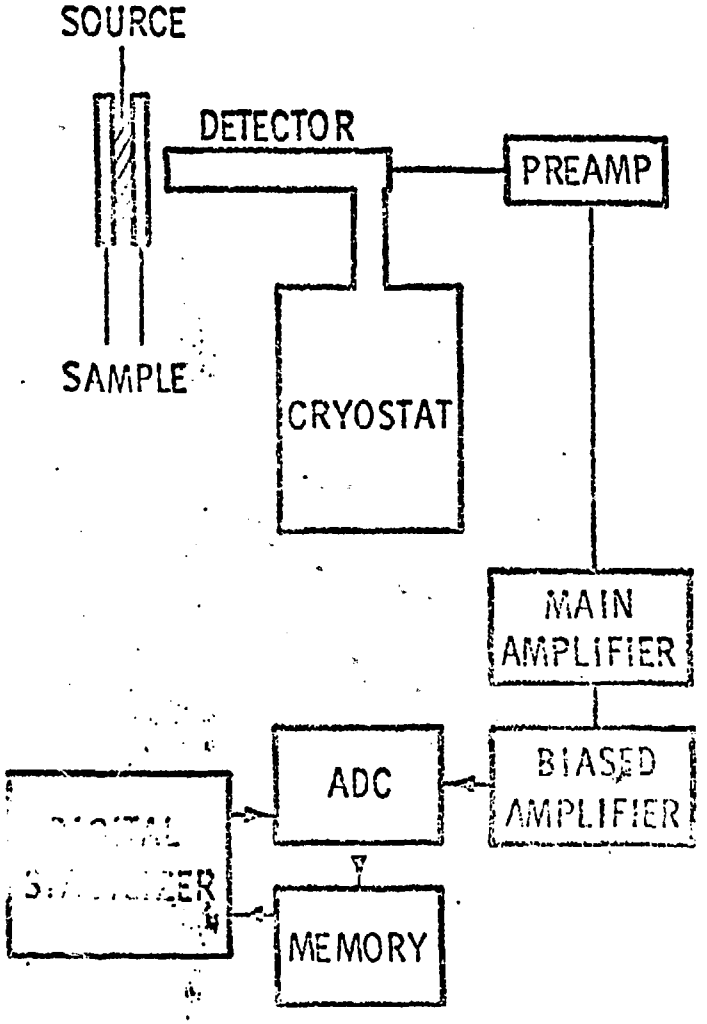

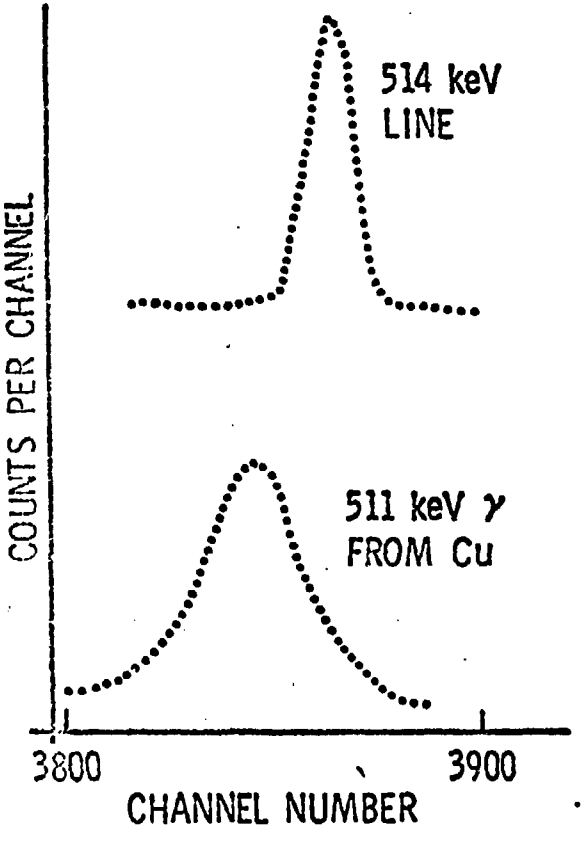

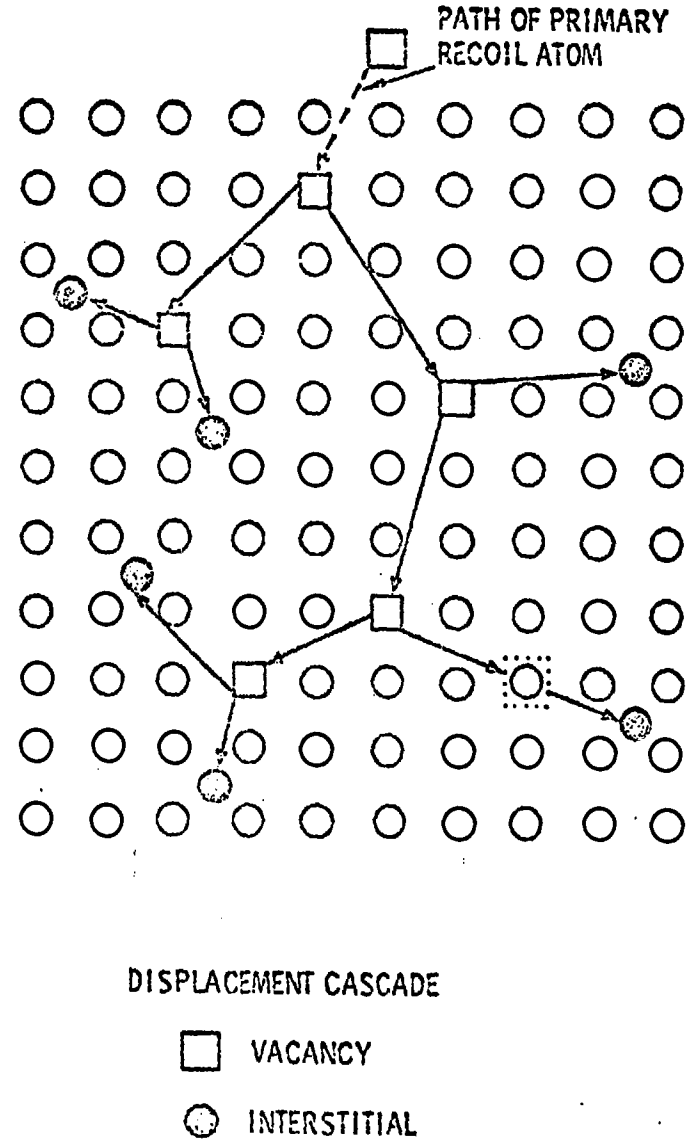
PATH OF PRIMARY
RECOIL ATOM
DISPLACEMENT CASCADE
VACANCY
INTERSTITIAL

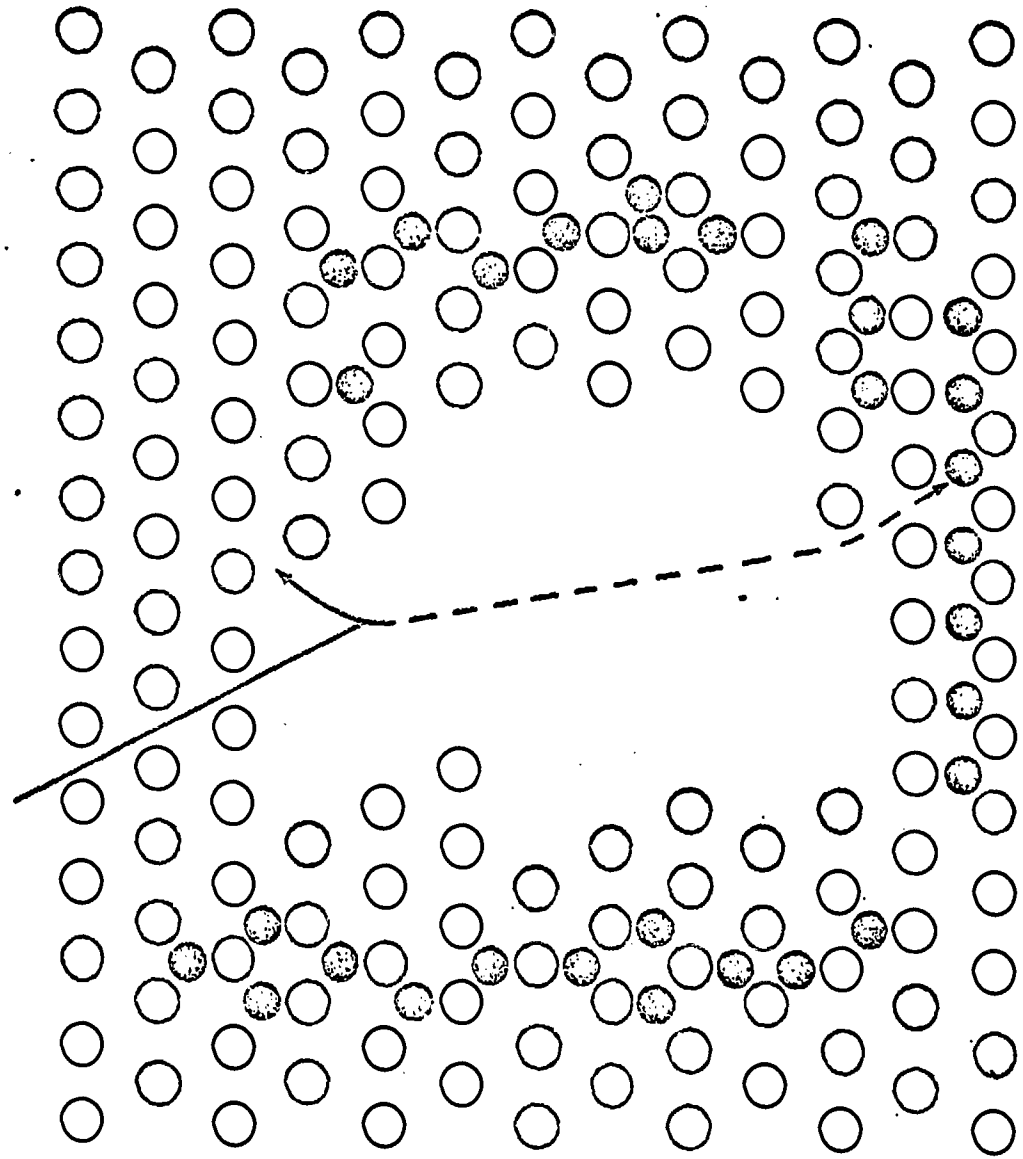

DISPLACEMENT SPIKE

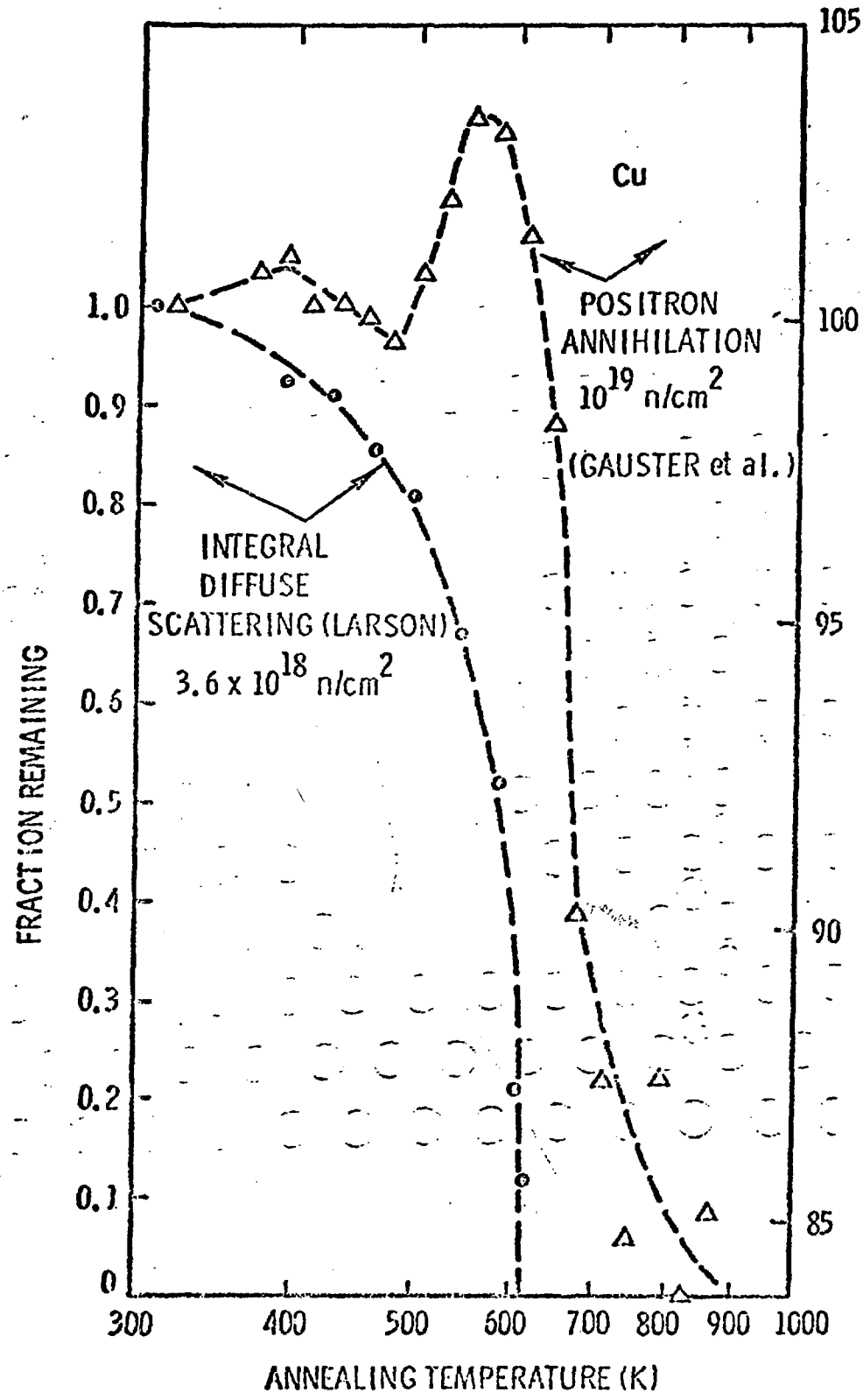
Cu
POSITRON ANNIHILATION
10^{19} n/cm^2
(GAUSTER et al.)
INTEGRAL DIFFUSE SCATTERING (LARSON)
3.6×10^{18} n/cm^2
FRACTION REMAINING
PEAK COUNT RATE (ARBITRARY UNITS)
ANNEALING TEMPERATURE (K)
1.0
0.9
0.8
0.7
0.6
0.5
0.4
0.3
0.2
0.1
0
105
100
95
90
85
300
400
500
600
700
800
900
1000